Bayesian Cramér-Rao Bound for Parameter Estimation Based on Mixed-Resolution Data

Yaniv Mazor, Itai E. Berman, and Tirza Routtenberg

Response to Reviewers' Comments

We would like to thank the Editor and the reviewers for their constructive comments and suggestions. In the following, we provide point-by-point responses to the comments of each reviewer, including the original review comments in italics, and details of our actions addressing these comments in blue font.

The **response to Reviewer 1's comments** is provided on Pages 2-6 of this letter and in the Appendix.

The **response to Reviewer 2's comments** is provided on Pages 7-14 of this letter.

Note: In the following, the numbered references (e.g., [29]) refer to the revised manuscript, and abbreviated references (e.g., [1-R]) refer to the bibliography included at the end of this response letter.

Abbreviations

ADC	analog to digital converter
CRB	Cramér-Rao Bound
BCRB	Bayesian CRB
BFIM	Bayesian Fisher information matrix
BZB	Bobrovsky-Zakai Bound
CDF	cumulative distribution function
LMMSE	linear minimum-mean-squared-error
MIMO	multiple-input multiple-output
MMSE	minimum mean-squared-error
MSE	mean-squared-error
PDF	probability density function
PMF	probability mass function
SNR	signal-to-noise ratio
WSN	wireless sensor network
WWB	Weiss-Weinstein Bound

Response to Reviewer 1's Comments

We thank Reviewer 1 for her/his comments and suggestions. Below, we provide our responses to each of the points raised.

1) **Comment:**
The positive:
-the derivation of the BCRB for mixed-resolution data is likely new.
The negatives:
The assumptions made are rather restrictive:
**H is a (semi)unitary matrix*
**G is also a (semi) unitary matrix with one unitary block repeated n˙q times*
**the two noises are white with known variances.*
In particular, under such conditions it is not surprising at all that the BCRB formula does not require a matrix inversion.

Our Response: We thank the reviewer for these comments, which gives us the opportunity to explain the motivation behind the considered model.
First, we would like to emphasize that the considered system model with the aforementioned assumptions has various applications and is widely used in the literature. In our previous work in [26], we showed that the following significant problems are special cases of this model:

- Scalar parameter estimation, which is widely used in WSNs (see e.g., [1], [9]). It is analytically shown in Section IV in [26] that this model satisfies our assumptions.
- Channel estimation in MIMO communication systems [25]–[30]. In Section V of [26] it is analytically shown that this model satisfies our assumptions.
- Sequential linear model, where measurements are taken over time with the same system matrices, but with possibly different ADC resolutions. Section V.A of [26] discusses this model's relevance extensively.

Many other applications use mixed-resolution data with similar assumptions on the system matrices, such as cognitive radio, array processing, source localization and target tracking, and general WSNs. In addition, the assumption of known noise variances is common in the relevant literature (see, e.g., [1-R], [1], [3], [5], [8]–[10], [15], [16], [19]- [30], [34]). Thus, the model and assumptions we use are both widely accepted in the research community and practical. The tractable form of the bound can, hence, be used for these applications. Second, it should be noted that, in addition to providing a mathematically tractable form of the bound for the considered case, the main aim of this work is to demonstrate and highlight the challenges of using the BCRB as a design tool for mixed-resolution data. Specifically, we demonstrate that resource allocation of the analog and quantized data cannot be effectively guided based on the mixed-resolution BCRB. These challenges appear even under the simpler model (i.e., with unitary matrices, white noise, and known noise variance) with the tractable form of the bound that does not need a matrix inversion. Thus, these assumptions are intended to facilitate the understanding of the readers, but the conclusions apply to the general case as well. In order to assure this claim we performed additional simulations for the general case, which are not presented here due to space limitations and the above-mentioned reasons. These simulations showed that the conclusions reached on the use of the mixed BCRB case for resource allocation are also valid for the general case.
To clarify the problem with resource allocation in the general case, it should be noted that, mathematically, the optimization of the BCRB for the general case (i.e., without the assumptions on the structure of the system matrices) results in an integer programming optimization. This can be seen

from the BFIM, which is now added to the paper and is given in (17). Determining the optimal number of analog and quantized measurements, N_a^* and N_q^*, respectively, by minimizing the inverse of (17) is impractical and may hinder insights into the problem. This is since the decision variables are the integers N_a and N_q that determine the dimensions of the matrices $\frac{1}{\sigma_a^2}\mathbf{H}^H\mathbf{H}$ and $\frac{1}{2\sigma_q^2}\mathbf{G}^H\mathbf{D}\mathbf{G}$, respectively. Thus, there is no simple way to solve the resource allocation in this case, and each value pair of the decision variables, N_a and N_q, requires the computation of the inverse of $\mathbf{J}$ and performing matrix multiplications, resulting in computational complexity of $O(M^3+2N_a^2M+2N_q^2M)$, which increases as the number of measurements increases. Therefore, in this work, we demonstrate the challenges of resource allocation via the BCRB under the assumptions of $\mathbf{H}$ and $\mathbf{G}$ (i.e., using the BCRB from (8)), which can be easily solved by simple optimization techniques, since the decision variables are the scalars n_a and n_q and no matrix inversion is needed.
To conclude, we chose to work under the considered assumptions because they are both commonly used (see the first point above) and lead to a tractable bound that can be used for optimization and resource allocation (see the second point above). We believe that this tractable form is highly useful for researchers in the field who are working on the aforementioned applications. In addition, for the sake of completeness and in response to this comment, we have developed the BCRB without these assumptions and included it in the paper (see the action below).

Our Action:
In response to the reviewer's comment, the following changes have been made:

- **Justification of the Model and the Assumptions:** In order to emphasize the applicability of the proposed model and justify the assumptions, we have added a description of relevant applications of the considered model in the first paragraph in Section II, and cited additional appropriate references (see [27], [28]). In particular, in Section II the justification for the model assumption has been expanded:
  "The considered model is applicable in various spheres, such as scalar estimation in sensor networks [1], [9], channel estimation in MIMO communications [25]–[30], and a sequential-time dynamic linear model with different data resolutions [26]. "
- **Highliting Assumptions in the Introduction:** It is now explicitly stated in the introduction (Page 1, Column 2) that the BCRB formula does not require a matrix inversion due to our assumptions: "We develop a closed-form expression of the mixed-resolution BCRB, which avoids matrix inversion due to the structure of the system matrices and the white noise assumption."
- **Integrating the General BCRB into the Bound Derivation:** To enable the use of our derivations for the general case (i.e., without the assumptions on the matrices), we have included the stages for the derivation of a more general form of the BCRB in the paper. We have also explicitly stated where we are using the properties of the matrices. The corresponding statement, which appears in Subsection III of the revised manuscript, is repeated below: "

$$\mathbf{J}_{\mathbf{x}_a|\boldsymbol{\theta}} = \frac{1}{\sigma_a^2}\mathbf{H}^H\mathbf{H} = \frac{\rho_a n_a}{\sigma_a^2}\mathbf{I}_M, \tag{14}$$

  where the last equality is obtained by substituting (2). In the supplemental material, it is shown that (13b) is reduced to

$$\mathbf{J}_{\mathbf{x}_q|\boldsymbol{\theta}} = \frac{1}{2\sigma_q^2}\mathbf{G}^H\mathbf{D}(\boldsymbol{\theta})\mathbf{G} = \frac{n_q}{2\sigma_q^2}\sum_{m=1}^{M} d_m(\boldsymbol{\theta})\mathbf{g}_m^*\mathbf{g}_m^T, \tag{15}$$

  where $\mathbf{D}(\boldsymbol{\theta}) = \text{diag}\left([d_1(\boldsymbol{\theta}),\cdots,d_M(\boldsymbol{\theta})]\right)$ and the last equality holds since $\mathbf{G}$ is a block matrix.

Overall, substituting (10), (12), (14), and (15) into (9) yields

$$\mathbf{J} = \left(1 + \frac{\rho_a n_a}{\sigma_a^2}\right)\mathbf{I}_M + \frac{n_q}{2\sigma_q^2}\sum_{m=1}^{M} \mathrm{E}_{\boldsymbol{\theta}}[d_m(\boldsymbol{\theta})]\mathbf{g}_m^* \mathbf{g}_m^T = \frac{1}{\rho_q}\mathbf{G}_1^H \left(\frac{\sigma_a^2 + \rho_a n_a}{\sigma_a^2}\mathbf{I}_M + \frac{\rho_q n_q}{2\sigma_q^2}\mathbf{D}\right)\mathbf{G}_1, \tag{16}$$

where $\mathbf{D} = \mathrm{E}_{\boldsymbol{\theta}}[\mathbf{D}(\boldsymbol{\theta})]$. For a non-singular $\mathbf{D}$, (16) implies the BCRB in (8). It should be noted that $\mathrm{E}_{\boldsymbol{\theta}}[d_m(\boldsymbol{\theta})]$ is analytically computed for $\tau = 0$, and is numerically evaluated for the general case. In addition, if $\mathbf{G}$ is not a block matrix, and (2) and (4) are not satisfied, then by substituting (10), (12), and the intermediate stages of (14) and (15) into (9) the BFIM in this case is

$$\mathbf{J} = \mathbf{I}_M + \frac{1}{\sigma_a^2}\mathbf{H}^H\mathbf{H} + \frac{1}{2\sigma_q^2}\mathbf{G}^H\mathbf{D}\mathbf{G}. \tag{17}$$

”

These changes aim to ensure that the assumptions and their implications are clear, while also providing a broader context for the applicability of the proposed model.

2) **Comment:** *Result (20) is implied by $BCRB_{pa} < BCRB$ (+), but it does NOT imply (+) (unless M=1), so your interpretation of (20) is not correct; instead of (20) you should have proved (+).*

Our Response: We thank the reviewer for this comment. The claim (Claim 1) and its proof have been revised accordingly. We believe that these changes significantly improve the clarity and accuracy of the mathematical derivation and presentation.

Our Action: Following the reviewer's comment, we added after the definitions in (6)-(7) the following clarification:
“The properties of the function $\frac{\phi^2(x)}{\Phi(x)\Phi(-x)}$ from (6) are discussed in [16].”
In addition, we enhanced the proof of Claim 1 in Section IV-B based on the properties of the function $d_n(\boldsymbol{\theta})$ and using [16]. The proof of this claim in the revised manuscript is repeated below for ease of reference:

Proof: “The inequality $\frac{\phi^2(x)}{\Phi(x)\Phi(-x)} \leq \frac{2}{\pi}$, $\forall x \in \mathbb{R}$ (see Eqs. (103)-(109) in [16]) implies that $d_n(\boldsymbol{\theta})$ from (6) satisfies

$$d_n(\boldsymbol{\theta}) \leq \frac{4}{\pi}, \quad \forall n = 1, \ldots, M, \quad \forall \boldsymbol{\theta} \in \mathbb{C}^M. \tag{22}$$

By using (16) and (20) and reorganizing, one obtains

$$\mathbf{J}_{pa} - \mathbf{J} = \frac{\rho_q n_q}{\sigma_q^2}\mathbf{I}_M - \frac{n_q}{2\sigma_q^2}\mathbf{G}_1^H\mathbf{D}\mathbf{G}_1 = \frac{n_q}{\sigma_q^2}\mathbf{G}_1^H(\mathbf{I}_M - \frac{1}{2}\mathbf{D})\mathbf{G}_1 \succeq \mathbf{0}, \tag{23}$$

where the second equality is obtained using the orthogonality in (4), and the last inequality is obtained since (22) implies that the diagonal matrix $\mathbf{I}_M - \frac{1}{2}\mathbf{D}$ has non-negative elements. Then, (23) implies that for non-singular BFIMs, $\mathbf{J}_{pa}$ and $\mathbf{J}$, the inequality in (21) holds.” ■

3) **Comment:** *The CR bounds are valid in the small estimation err regime. For binary data it is a well-known fact that the noise has a dithering effect, the implication being that beyond a certain SNR value the mse grows and hence departs from the CR bound as the SNR increases. Therefore, the behavior illustrated in your Fig 1 was quite expected. In your case with $M = 1$ (just one unknown parameter) and in the high SNR case, a simple LS estimate using only the analog data would perform better than the LMMSE (the Bayesian prior induces a bias in your estimate, and it is not needed in this well-conditioned case, and the use of binary data in the high SNR case increases both the bias and variance of your estimate).*

Our Response: We thank the reviewer for this comment. Our response is as follows:

- **Dithering and Resource Allocation:** Indeed, the behavior illustrated in our simulations aligns with the expected dithering effect, which is well-known for quantized data. These outcomes demonstrate the validity of the proposed formula of the mixed-resolution BCRB. In addition, our simulations are the first to show that in the mixed-resolution case, the BCRB does not accurately reflect the behavior of the estimators in terms of resource allocation. That is, as demonstrated in Figs. 1a and 1b, the relative performance of different resource allocation policies varies across SNR regions, but the mixed-resolution BCRB does not predict this phenomenon. Thus, while the BCRB is widely used in the literature for system design (see e.g., [2-R], [16]- [22]) our simulation results suggest that it cannot be used as a design tool for the resource allocation problem.
- **Alternative Estimators:** It should be noted that in our case, a simple LS estimator using only the analog data would perform similarly to the LMMSE and the MMSE estimators in the high SNR regime. This is illustrated in the following figure, Fig. I. We decided not to include this estimator in order to avoid confusion, as our focus is on the Bayesian model, which is commonly used in the mixed-resolution case (see e.g., [25]–[27], [29], [30]), while the LS estimator was developed for the non-Bayesian estimation of a deterministic unknown parameter. Further, based on the reviewer's comment, we have included the MMSE estimator in our simulations. Generally, the MMSE estimator has a lower MSE than the LMMSE estimator, and both estimators coincide in the high SNR regime (due to the linear Gaussian case for the analog measurements). Thus, the revised figures in the paper now include the MMSE estimator, demonstrating that the non-monotonic behavior w.r.t. the resource allocation setting occurs for different estimators. It can be seen in the revised figures in the paper that, since in the high SNR regime the LMMSE estimator relies solely on analog observations, its results coincide with those of the MMSE estimator, since we obtain the linear Gaussian case for the analog measurements. We believe that the new simulations and the associated conclusions elucidate the conclusion in the manuscript, and we thank the reviewer for this point.

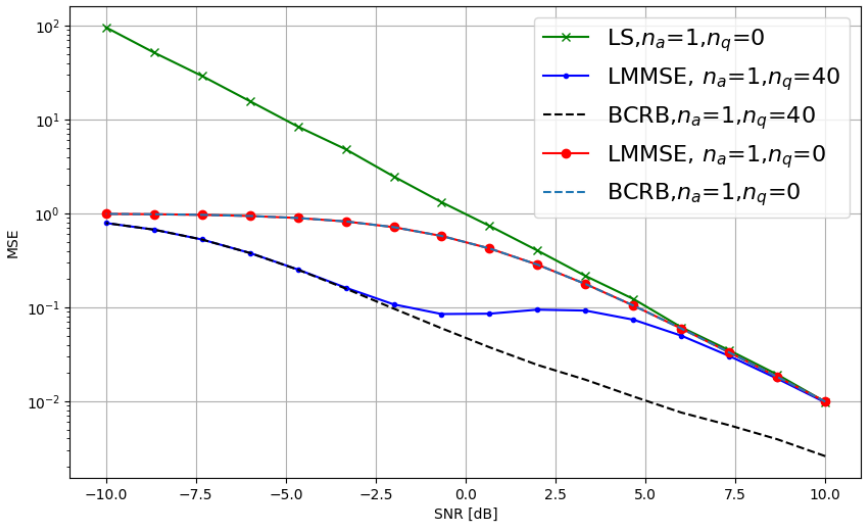

Fig. I: LS estimator using only analog data, in comparison to mixed and analog LMMSE and the BCRB. As a result of the well-known dithering effect, all the estimators coincide in the high SNR region.

Our Action:

- We emphasize in the abstract, introduction, and conclusion that the resource allocation problem

is the main new issue demonstrated here (in addition to the known dithering effect). The changes appear below for ease of reference:

- Abstract: "Moreover, the mixed-resolution BCRB fails to accurately capture the non-monotonic behavior of the estimators' MSEs versus signal-to-noise-ratio (SNR) and their behavior regarding different resource allocations. Consequently, while the BCRB provides some valuable insights, it requires careful examination before being used as a tool for system design in these scenarios."
- Introduction (Page 1, End of column 2): "Finally, we show via simulations that while the BCRB provides some valuable insights, it cannot serve as a system design tool for setting the resource allocation."
- Conclusion: "Simulation results show that the BCRB for mixed-resolution data is unachievable by the MMSE and the LMMSE estimators outside the low SNR region, does not capture the non-monotonic behavior of the MSE versus SNR, and, hence, is not a suitable tool for optimizing the resource allocation."

- We added the MMSE estimator to all simulations. The results are presented in Figs. 1a and 1b. The discussion of these figures now includes the MMSE estimator.

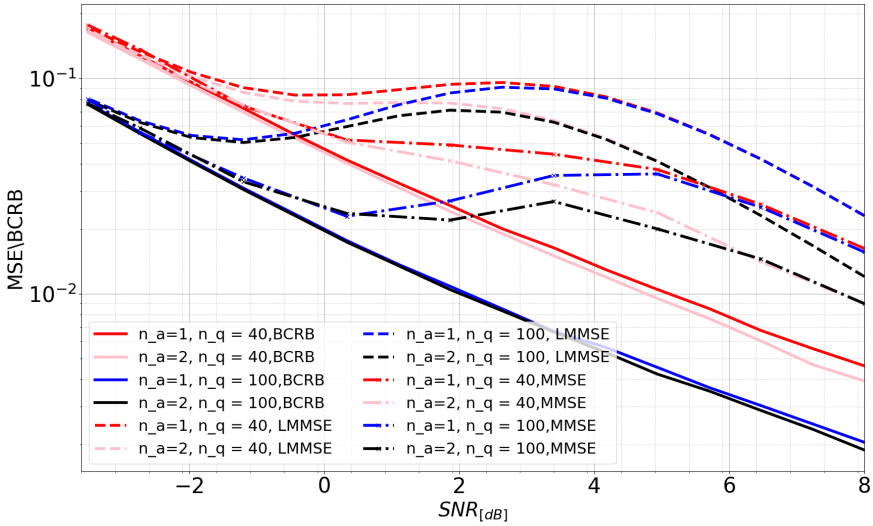

Fig. II: (Fig. 1a of the revised manuscript) The BCRB and MSE of the estimators (a) versus SNR

"It can be seen that the MSEs of both estimators are not monotonic decreasing functions of the SNR, while the BCRB monotonically decreases as the SNR decreases."
In the explanations of the simulations, we added:
"for high a SNRs, the estimators rely solely on the analog observations and, thus, coincide (and are also equal to the analog-data least squared estimator). The BCRB does not capture the region where the quantized data becomes non-informative."

Response to Reviewer 2's Comments

We thank Reviewer 2 for the valuable comments and suggestions. Below, we provide our responses to each of the points raised.

1) **Comment:** *In the manuscript, the PCRB is derived for an interesting and important problem. The main message is, however, disappointing: the authors derived the bound but also they claim that it is useless. Actually, they only proved that the partially numeric LMMSE estimator in section V has a variance higher than PCRB.*
I am not sure if the manuscript deserves to be published. Should the journal publish an useless bound ? But still, I like the paper and I am in favor. Maybe you only should delete the disqualifying remark that the PCRB s an inappropriate tool for system design. BTW, PCRB is not the only bound, and definitely not the tightest one.

Our Response: We thank the reviewer for this comment and for the overall positive feedback. Based on the Editor's decision to encourage a resubmission, we understand that the manuscript fits the journal's publication policy. In addition, we would like to take this opportunity to explain why we believe these results are important and should be shared with the signal-processing community.

We agree that the remark about the BCRB being an inappropriate tool for system design was disqualifying and did not fully consider the potential usefulness of the BCRB in other contexts. For example, the mixed-resolution BCRB has reasonable behavior w.r.t. the threshold (see Fig. 1b in the paper). Therefore, we have revised the text to present a more balanced view. However, we still believe that it is crucial to convey the message that the BCRB may not always be suitable as the tool for system design, especially in non-trivial, non-linear settings. In a domain where performance bounds frequently serve as benchmarks or tools for system design, highlighting the limitations of the BCRB in this context is important for researchers. This will enable proper tool selection for these mixed-resolution applications (for example, in cases where it is possible to optimize the resource allocation based on the MSE of a specific estimator). We also hope that this finding will challenge researchers to develop alternative bounds for this problem.

Regarding tighter bounds: we acknowledge the significance of establishing tighter bounds for the mixed-resolution case. However, developing these large-error bounds (e.g., WWB and BZB) is complex and beyond the scope of the current manuscript. Moreover, it may not solve the problem of the monotonic behavior of the bounds w.r.t. SNR and the behavior w.r.t. resource allocation. This is because these bounds are also based on the PMF of the quantized data, rather than PDF used in the continuous random parameter estimation.

Our Action: In response to this comment, the following changes have been made:

- We deleted the following disqualifying remark: "Our simulation results also show that the BCRB is an inappropriate tool for system design (e.g., threshold setting) and resource allocation."
- We revised the abstract, introduction, and conclusion to provide a more balanced view of the BCRB's applicability and to emphasize the need for careful consideration with regard to its use in practical applications. We now state that while the BCRB may be useful for certain purposes and provide some insights, it is not suitable for resource allocation. The changes appear below for ease of reference:
  - Abstract: "Moreover, the mixed-resolution BCRB fails to accurately capture the non-monotonic behavior of the estimators' MSEs versus signal-to-noise-ratio (SNR) and their behavior regarding different resource allocations. Consequently, while the BCRB provides some valuable insights, it requires careful examination before being used as a tool for system design in these scenarios."

  - Introduction (Page 1, End of column 2): "Finally, we show via simulations that while the BCRB provides some valuable insights, it cannot serve as a system design tool for setting the resource allocation."
  - Conclusion: "Simulation results show that the BCRB for mixed-resolution data... is not a suitable tool for optimizing the resource allocation."
- We added to the conclusion the importance of exploring tighter bounds as a future research direction:
  "Future research should address tighter, large-error bounds for realistic performance analysis and effective system design. "

2) **Comment:** *Is the LMMSE estimator equivalent to* $\mathrm{E}[\boldsymbol{\theta}|\mathbf{x}]$*? If not, then the gap between the variance of* $\mathrm{E}[\boldsymbol{\theta}|\mathbf{x}]$ *and the PCRB can be smaller, it can be monotonic with respect to (w.r.t.) SNR, etc. Why not? Did you prove the opposite?*

Our Response: We thank the reviewer for this comment. Indeed, the MMSE estimator generally has a lower MSE than the LMMSE estimator, and these estimators are not identical in the considered non-linear case outside the asymptotic region of high SNR.
The MMSE estimator of $\boldsymbol{\theta}$ based on the mixed-resolution data $\mathbf{x}_a$ and $\mathbf{x}_q$, $\mathrm{E}[\boldsymbol{\theta}|\mathbf{x}] = \mathrm{E}[\boldsymbol{\theta}|\mathbf{x}_a, \mathbf{x}_q]$, and its associated MSE do not possess closed-form analytical expressions in this case. This is due to the fact that the conditional PDF, $p(\boldsymbol{\theta}|\mathbf{x})$, is intractable in the presence of quantized measurements. Furthermore, for high-dimensional $\boldsymbol{\theta}$, i.e., a large value of M, the numerical evaluation of the MMSE estimator via multidimensional integration is impractical for mixed-resolution measurements. Hence, the LMMSE estimator is usually used with quantized measurements. This was our original intention in presenting the LMMSE estimator.
However, we agree with the reviewer that in the considered setting of our simulations, the MMSE estimator can be numerically evaluated (since $M = 1$) and added to the simulations. Thus, in accordance with this comment, we added the MMSE estimator to the simulations, utilizing numerical calculations of $\mathrm{E}[\boldsymbol{\theta}|\mathbf{x}]$. It can be seen that while the gap between the MSE of $\mathrm{E}[\boldsymbol{\theta}|\mathbf{x}]$ and the BCRB is smaller than those of the LMMSE estimator, the main conclusions remain consistent with those for the LMMSE estimator. Specifically, the MSE is non-monotonic w.r.t. SNR, the relative performance of different resource allocation policies varies across SNR regions, and the BCRB does not predict these phenomena. These outcomes demonstrate the validity of the aforementioned principles for both the LMMSE and MMSE estimators. Another interesting point is that the optimal resource allocation policy depends on the estimator that is used, with different behaviors observed for each estimator. For example, it can be seen in Fig. 1a that for an SNR of 3_{dB}, the best policy for the LMMSE estimator among the presented policies is $(n_a, n_q) = (2, 40)$, while for the MMSE estimator, the policy of $(n_a, n_q) = (2, 100)$ is preferable at this SNR. Finally, it can be seen that in the high SNR regime, the LMMSE estimator relies solely on analog observations and, thus, coincides with the MMSE estimator since we obtain the linear Gaussian case for the analog measurements.
We believe that the new simulations and the associated conclusions enhance our manuscript. We are grateful to the reviewer for these useful additions.

Our Action: Based on this comment, we have added the performance of the MMSE estimator, $\mathrm{E}[\boldsymbol{\theta}|\mathbf{x}]$, to our simulations. We also keep the presentation of the LMMSE estimator, since 1) this is the commonly used estimator for mixed-resolution estimation; 2) the LMMSE estimator is also applicable for larger values of M; and 3) the comparison between the performance of these estimators w.r.t. different resource allocation policies provides important insights.
The changes appear in Fig. 1 (see below) and are discussed in Section VI.

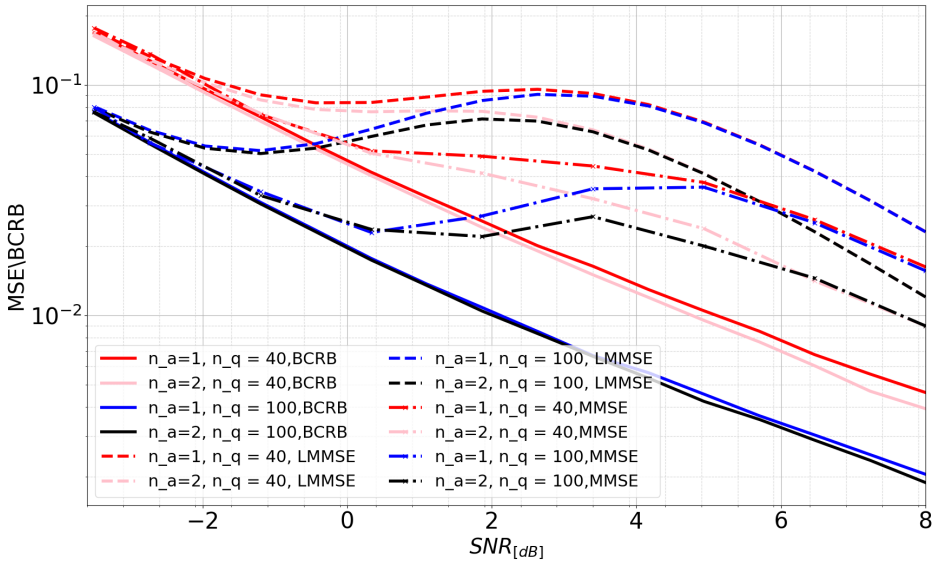

(a)

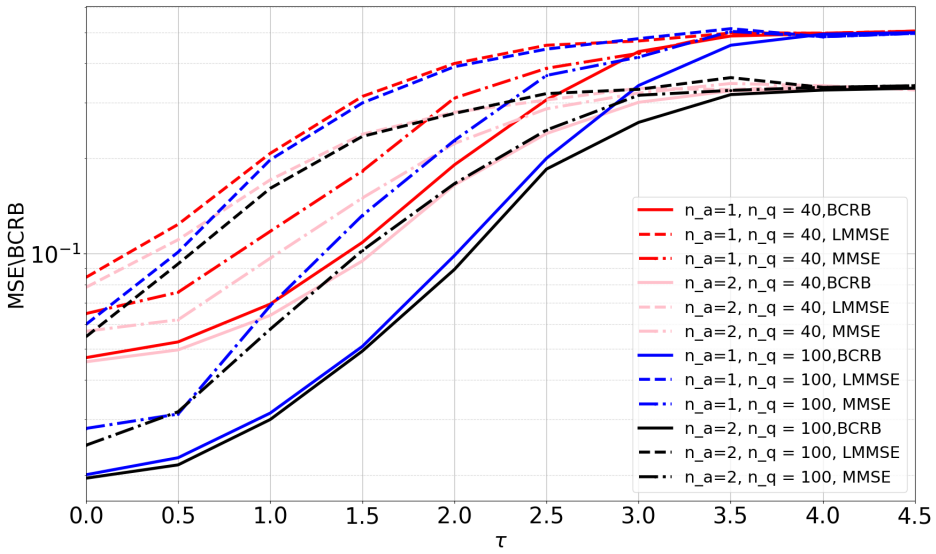

(b)

Fig. III: (Fig. 1 of the revised manuscript) The BCRB and MSE of the estimators (a) versus SNR for $\boldsymbol{\tau} = \mathbf{0}$; and (b) versus τ for SNR=0_{dB}.

3) **Comment:** *End of Introduction: why the PCRB is asymptotically achievable by the LMMSE estimator? I'd like to see the proof. I do not think that this statement is true.*

Our Response: We agree with the reviewer and apologize for the incorrect statement. Our original intention was to refer specifically to the analog-data-only case, but we agree that this is redundant and potentially confusing.

Our Action: We have removed this sentence in the revised version.

4) **Comment:** *In (6), d_n is random because it is a function of the random theta. Maybe it would be good to write it as $d_n(\boldsymbol{\theta})$.*
g_n introduced after (6) is not seen in (6). It appears in (7), so I suggest to introduce it after (7).

Our Response: We thank the reviewer for this comment, and accept these suggestions.

Our Action: The following changes have been made:

- We changed the notation of d_n to $d_n(\boldsymbol{\theta})$ in (6), and throughout the paper.
- We moved the sentence with the definition of $\mathbf{g}_n$ to be located after (7) in the revised version.

5) **Comment:** *In (8), I think that there is missing a matrix inversion. PCRB should be inversion of the FIM. So please correct. The same error is probably in (18).*

Our Response: We would like to emphasize that under the described model, where $\mathbf{G}$ is a block matrix, the bound is computed without the need for matrix inversion. Thus, there is no error in (18). This can be shown as follows.
The BFIM present in (16) is equal to

$$\mathbf{J} = \frac{1}{\rho_q}\mathbf{G}_1^H \left(\frac{\sigma_a^2 + \rho_a n_a}{\sigma_a^2}\mathbf{I}_M + \frac{\rho_q n_q}{2\sigma_q^2}\mathbf{D} \right) \mathbf{G}_1. \tag{L1}$$

The inverse of a multiplication of non-singular square matrices satisfies $(\mathbf{A}_1\mathbf{A}_2\mathbf{A}_3)^{-1} = \mathbf{A}_3^{-1}\mathbf{A}_2^{-1}\mathbf{A}_3^{-1}$ (p. 24 [3-R]). Thus, in our case

$$\mathbf{J}^{-1} = \rho_q \mathbf{G}_1^{-1} \left(\frac{\sigma_a^2 + \rho_a n_a}{\sigma_a^2}\mathbf{I}_M + \frac{\rho_q n_q}{2\sigma_q^2}\mathbf{D} \right)^{-1} \mathbf{G}_1^{H^{-1}}. \tag{L2}$$

Since according to our model (section II), $\mathbf{G}_1$ is a square unitary matrix (scaled by ρ_q), i.e.

$$\mathbf{G}_1^H \mathbf{G}_1 = \rho_q \mathbf{I}_M, \tag{4}$$

then

$$\mathbf{G}_1^{-1} = \frac{1}{\rho_q}\mathbf{G}_1^H, \quad \mathbf{G}_1^{H^{-1}} = \frac{1}{\rho_q}\mathbf{G}_1. \tag{L3}$$

In addition, $\left(\frac{\sigma_a^2 + \rho_a n_a}{\sigma_a^2}\mathbf{I}_M + \frac{\rho_q n_q}{2\sigma_q^2}\mathbf{D} \right)$ is a diagonal matrix, and therefore, its inverse is given by

$$\left(\frac{\sigma_a^2 + \rho_a n_a}{\sigma_a^2}\mathbf{I}_M + \frac{\rho_q n_q}{2\sigma_q^2}\mathbf{D} \right)^{-1} = \left(\frac{\sigma_a^2}{\sigma_a^2 + \rho_a n_a}\mathbf{I}_M + \frac{2\sigma_q^2}{\rho_q n_q}\mathbf{D}^{-1} \right), \tag{L4}$$

where $\mathbf{D}^{-1} = \text{diag}\left([\frac{1}{\mathrm{E}_{\boldsymbol{\theta}}[d_1(\boldsymbol{\theta})]}, \cdots, \frac{1}{\mathrm{E}_{\boldsymbol{\theta}}[d_m(\boldsymbol{\theta})]}] \right)$.
By substituting (L3) and (L4) in (L2) we obtain

$$\mathbf{J}^{-1} = \rho_q \frac{1}{\rho_q}\mathbf{G}_1^H \left(\frac{\sigma_a^2}{\sigma_a^2 + \rho_a n_a}\mathbf{I}_M + \frac{2\sigma_q^2}{\rho_q n_q}\mathbf{D}^{-1} \right) \frac{1}{\rho_q}\mathbf{G}_1, \tag{L5}$$

which implies, after reordering, that:

$$BCRB = \mathbf{J}^{-1} = \frac{1}{\rho_q}\mathbf{G}_1^H \left(\frac{\sigma_a^2}{\sigma_a^2 + \rho_a n_a}\mathbf{I}_M + \frac{2\sigma_q^2}{\rho_q n_q}\mathbf{D}^{-1} \right) \mathbf{G}_1. \tag{L6}$$

The BCRB in (L6) reduces to the expression in eq. (8).

6) **Comment:** *Notation. In (11) we have $p(x|\theta)$, in (13a) there is $f(x_a|\theta)$. A conditional PDF at the end of section II is denoted $f(\theta|x)$. Please unify these notations somehow, or, at least, explain what is $p(x|theta)$ in (11). The notation Pr$(x_q|\theta)$ in (13b) was not explained.*

Our Response: We thank the reviewer for pointing out these inconsistencies.

Our Action: Following the reviewer's comment, we have unified the notation. In the revised version (both in the paper and in the supplemental material), we denote the different PDFs, PMFs, and their mixed version by $p(\cdot)$. Additionally, we clarified the notation in Footnote 1 (Page 2):
"For the sake of simplicity, we denote both PDF, probability mass function (PMF), and their mixed version by p."
We have also updated the notations accordingly after Eqs. (13a), (13b), at the end of Section II, and in the supplemental material.

7) **Comment:** *What is the n in the limit in (24)*

Our Response: The n notation represents n_q and n_a that both go to infinity.

Our Action: We replaced $n \to \infty$ in (26) with $n_q, n_a \to \infty$, as in (25).

8) **Comment:** *End of page 3. Here, it says that mu is the expected value, but does not say expected value of what. Next, the notation mu_an and mu_b remain undefined. Is mu_a the same as mu_{x_a}?*

Our Response: We agree that this notation was confusing, and we realized that we could use the expectation operator instead.

Our Action: In order to avoid confusion, we changed this notation. In particular, the revised version in the first paragraph of Section V now reads:
"...Since in the considered model $\boldsymbol{\theta}$ has a zero mean, the analytical LMMSE estimator is

$$\hat{\boldsymbol{\theta}} = \mathbf{C}_{\boldsymbol{\theta}\mathbf{x}}\mathbf{C}_{\mathbf{x}}^{-1}(\mathbf{x} - \mathrm{E}[\mathbf{x}]), \tag{29}$$

where for the mixed-resolution case,

$$\mathbf{C}_{\mathbf{x}} = \begin{bmatrix} \mathbf{C}_{\mathbf{x}_a} & \mathbf{C}_{\mathbf{x}_a\mathbf{x}_q} \\ \mathbf{C}_{\mathbf{x}_q\mathbf{x}_a} & \mathbf{C}_{\mathbf{x}_q} \end{bmatrix}, \quad \mathbf{C}_{\boldsymbol{\theta}\mathbf{x}} = \begin{bmatrix} \mathbf{C}_{\boldsymbol{\theta}\mathbf{x}_a} & \mathbf{C}_{\boldsymbol{\theta}\mathbf{x}_q} \end{bmatrix}, \tag{30}$$

and $\mathrm{E}[\mathbf{x}] = [\mathrm{E}[\mathbf{x}_a]^T, \mathrm{E}[\mathbf{x}_q]^T]^T$. We use the notation of the auto- and cross-covariance matrices of complex-valued vectors $\mathbf{a}$ and $\mathbf{b}$ as $\mathbf{C}_{\mathbf{a}} \triangleq \mathbf{C}_{\mathbf{aa}}$ and $\mathbf{C}_{\mathbf{ab}} \triangleq \mathrm{E}[(\mathbf{a} - \mathrm{E}[\mathbf{a}])(\mathbf{b} - \mathrm{E}[\mathbf{b}])^H]$."

9) **Comment:** *Function $\mathrm{E}_{\boldsymbol{\theta}}[d_n]$ seems to be function of two parameters only: tau and m. Could the authors compute this function numerically and present a figure showing how it looks like in mesh*

Our Response: We thank the reviewer for this comment. The function $d_n(\boldsymbol{\theta})$ in (6) consists of the contributions of the real and imaginary parts, and is based on the function:

$$\frac{\phi^2(x)}{\Phi(x)\Phi(-x)}, \quad x \in \mathbb{R}. \tag{L7}$$

This function is presented in Fig. IV below. It can be seen that this is a unimodal non-negative function, whose maximum is attained at $x = 0$. This function and its properties are discussed in [16]. In particular, it is shown in [16] that the maximum value is $\frac{2}{\pi}$.
The function $\mathrm{E}_{\boldsymbol{\theta}}[d_n(\boldsymbol{\theta})]$, derived from (L7) above, constitutes the non-analytic component of the BCRB, and its behavior directly influences the characteristics and properties of the bound. In response to the reviewer's request, we have computed this function numerically and present it in Fig. V. This figure illustrates the function's appearance in a mesh plot w.r.t. τ and σ_q. We see that the function is indeed bounded by $\frac{4}{\pi}$ and decreases as its absolute value argument (7) grows. However, due to space limitations, we did not include these figures in the paper.

Our Action: Following this comment, we added the following clarification after (6):
"The properties of the function $\frac{\phi^2(x)}{\Phi(x)\Phi(-x)}$ from (6) are discussed in [16]."

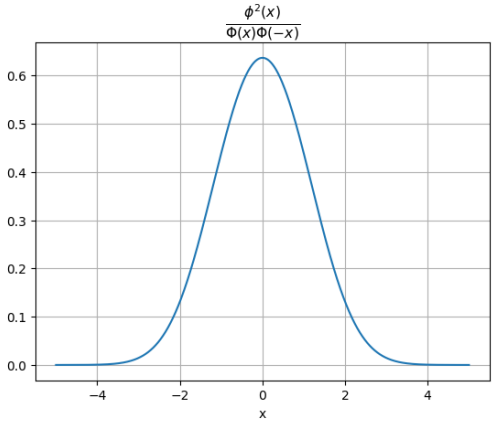

Fig. IV: The generating function of $d_n(\boldsymbol{\theta})$

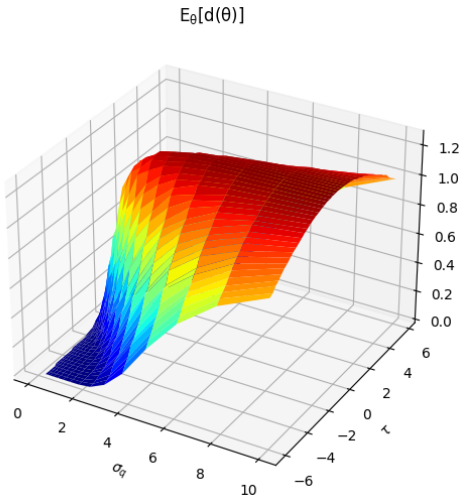

Fig. V: Mesh look of $\mathrm{E}_{\boldsymbol{\theta}}[\mathrm{d_n}(\boldsymbol{\theta})]((6))$ as function of σ_q and τ.

In addition, we revised the proof of Claim 1 in Section IV-B based on the properties of the function $d_n(\boldsymbol{\theta})$ referring to [16]. In particular, the proof of Claim 1 is now based on an upper bound on the function from (L7) above that is derived in [16]. The revised proof of this claim is as follows:

Proof: "The inequality $\frac{\phi^2(x)}{\Phi(x)\Phi(-x)} \leq \frac{2}{\pi}$, $\forall x \in \mathbb{R}$ (see Eqs. (103)-(109) in [16]) implies that $d_n(\boldsymbol{\theta})$ from (6) satisfies

$$d_n(\boldsymbol{\theta}) \leq \frac{4}{\pi}, \quad \forall n = 1, \ldots, M, \quad \forall \boldsymbol{\theta} \in \mathbb{C}^M. \tag{22}$$

By using (16) and (20) and reorganizing, one obtains

$$\mathbf{J}_{pa} - \mathbf{J} = \frac{\rho_q n_q}{\sigma_q^2}\mathbf{I}_M - \frac{n_q}{2\sigma_q^2}\mathbf{G}_1^H \mathbf{D}\mathbf{G}_1 = \frac{n_q}{\sigma_q^2}\mathbf{G}_1^H(\mathbf{I}_M - \frac{1}{2}\mathbf{D})\mathbf{G}_1 \succeq \mathbf{0}, \tag{23}$$

where the second equality is obtained using the orthogonality in (4), and the last inequality is obtained since (22) implies that the diagonal matrix $\mathbf{I}_M - \frac{1}{2}\mathbf{D}$ has non-negative elements. Then, (23) implies that for non-singular BFIMs, $\mathbf{J}_{pa}$ and $\mathbf{J}$, the inequality in (21) holds." ■

10) **Comment:** *Table with Algorithm 1 contains a diagonal loading. This was not mentioned in the main text. How the parameter ϵ is taken*

Our Response: The parameter ϵ can be selected in different ways, typically involving the choice of "small" values relative to the values in the simulation. In our simulations, we set ϵ to the standard deviation of the eigenvalues of $\hat{\Delta}$, as proposed in [35].

Our Action: In response to this comment, the following changes have been made:

- We added the following sentence after (32):
  "To avoid numerical stability issues, we add the commonly-used diagonal loading [35] prior to inverting the estimated matrix $\hat{\boldsymbol{\Delta}}$."
- We now clarified how ϵ was chosen in our simulations:
  "... where ϵ is the standard deviation of the eigenvalues of $\hat{\Delta}$, as in [35]."

11) **Comment:** *Figure 1b contains an acronym PMLE which was not explained. It seems from the figure caption that it is the same thing as in the diagram (a). Why the notation in the lower diagram is different*

Our Response: We thank the reviewer for pointing out this typo.

Our Action: We removed the acronym from Fig. 1b, and refer to it as the LMMSE estimator:
"In this section, we numerically evaluate the behavior of the BCRB from (8) *and compare it with the MSE of: 1) the MMSE estimator, evaluated via numerical integration; and 2) the LMMSE estimator implemented as in [26] for $\boldsymbol{\tau} = \mathbf{0}$, and by Algorithm 1 otherwise..."*

12) **Comment:** *Why the curves in Fig. 1a have sharp edges at tau=2 and tau=5 ? It is suspicious. Do you have any explanation to this phenomenon, or it is an error ?*

Our Response: We thank the reviewer for this comment. Upon reviewing our proof, we discovered an error involving the $\sqrt{\ }$ factor, which we promptly corrected. The mathematical correction has led to graphs that appear more sensible, without sharp edges. Thanks to the reviewer, we now present more sensible and reliable results. These results indicate the reversal in the performance of the estimators (Fig. 1.b of the revised manuscript), depending on their resource allocation partition. This reversal occurs for relatively large values of τ, rendering the bounds irrelevant for solving the resource allocation problem.

Our Action: We corrected the expected value of x_{q_n} in the beginning of section S.III, and revised eq. (S-11),(S-12) in the supplemental material:
"The expected value of x_{q_n} is $\frac{1}{\sqrt{2}}\left(\left(1-2\overline{P_1}\right)+j\left(1-2\overline{P_2}\right)\right)$, where

$$\overline{P_1} = \Pr(\mathrm{Re}(\mathbf{g}_n^T\boldsymbol{\theta}) + \mathrm{Re}(w_n) - \tau_n^R < 0), \tag{S-9}$$

$$\overline{P_2} = \Pr(\mathrm{Im}(\mathbf{g}_n^T\boldsymbol{\theta}) + \mathrm{Im}(w_n) - \tau_n^I < 0). \tag{S-10}$$

Then, using the Gaussianity of the different terms, it can be verified that $\overline{P_1} = \Phi(\frac{\tau_n^R - \tilde{\mu}_R}{\tilde{\sigma}_R})$, where $\tilde{\mu}_R$ and $\tilde{\sigma}_R$ are the mean and the standard deviation of $\mathrm{Re}(\mathbf{g}_n^T\boldsymbol{\theta}) + \mathrm{Re}(u_n)$, respectively. Similarly, we can compute $\overline{P_2}$ via the distribution of $\mathrm{Im}(\mathbf{g}_n^T\boldsymbol{\theta}) + \mathrm{Im}(u_n)$. Based on our model from Section II, we get

$$\tilde{\mu}_R = \tilde{\mu}_{Im} = 0, \quad \tilde{\sigma}_R^2 = \tilde{\sigma}_I^2 = \frac{1}{2}(\sigma_q^2 + \rho_q). \tag{S-11}$$

Eventually, taking (S-11) into account, we get

$$\sqrt{2}\mathrm{E}[x_{q_n}] = \left(1 - 2\Phi(\frac{\tau_n^R}{\sqrt{\frac{1}{2}(\sigma_q^2 + \rho_q)}})\right) + j\left(1 - 2\Phi(\frac{\tau_n^{Im}}{\sqrt{\frac{1}{2}(\sigma_q^2 + \rho_q)}})\right). \tag{S-12}$$

”

REFERENCES

[1-R] Jacobsson, Sven and Durisi, Giuseppe and Coldrey, Mikael and Gustavsson, Ulf and Studer, Christoph ”Throughput analysis of massive MIMO uplink with low-resolution ADCs” *IEEE Trans. Wireless Communications*, 2017

[2-R] Saska, David and Blum, Rick S and Kaplan, Lance ”Fusion of Quantized and Unquantized Sensor Data for Estimation” *IEEE Signal Processing Letters*, 2015

[3-R] K. HOFFMAN, R. Kunze ”LINEAR ALGEBRA ” ,second edition,Prentice Hall,1971

,